Journal of Inorganic Biochemistry 196 (2019) 110687

Contents lists available at ScienceDirect

Journal of Inorganic Biochemistry

journal homepage: www.elsevier.com/locate/jinorgbio

Synergistic antibacterial mechanism of Bi_2Te_3 nanoparticles combined with the ineffective β-lactam antibiotic cefotaxime against methicillin-resistant *Staphylococcus aureus*

Xiangyu Liu[a], Lulu Ma[a], Fan Chen[a], Junzi Liu[a,b], Hao Yang[a], Zhong Lu[a,*]

[a] Research Center for Environmental Ecology and Engineering, School of Environmental Ecology and Biological Engineering, Wuhan Institute of Technology, No. 206, Guanggu First Road, Wuhan 430073, PR China
[b] Hubei Three Gorges Polytechnic, Yichang, 443000, Hubei, PR China

ARTICLE INFO

Keywords:
Bi_2Te_3 nanoparticles
Cefotaxime
Methicillin-resistant *Staphylococcus aureus*
Synergistic antibacterial effect
Mechanism

ABSTRACT

Methicillin-resistant *Staphylococcus aureus* (MRSA) infections have become a serious threat to public health because traditional antibiotics are less efficient. Here, we developed a simple and efficient combination of Bi_2Te_3 nanoparticles (NPs) with β-lactam antibiotics cefotaxime (CTX), which presented significant synergistic antibacterial activity against MRSA. The minimal inhibitory concentration of CTX decreased from 256 to 32 μg/mL in the presence of 8 μg/mL Bi_2Te_3 NPs. The results of cell membrane potential and cellular K^+ content measurements demonstrated that the destruction of membrane functions is a factor in the synergistic mechanism. Furthermore, the induction of cellular reactive oxygen species generation, inhibition of β-lactamases induced by CTX and direct damage to the cell structure constituted other factors of the synergistic mechanism. These observations suggest that reviving the efficacy of ineffective β-lactam antibiotic CTX by Bi_2Te_3 NPs may be a potentially effective therapeutic strategy to overcome refractory MRSA infections.

1. Introduction

Multidrug-resistant (MDR) pathogens pose a substantial threat to public health [1–3]. Methicillin-resistant *Staphylococcus aureus* (MRSA) is one of the most prevalent MDR pathogens worldwide, causing pneumonia, skin infection, osteomyelitis and bacteremia and exhibiting remarkable resistance to multiple antibiotic treatments [4–8]. However, the development of new antibiotics is vastly outpaced by current therapies that are losing efficacy [9–12].

Compared with developing monotherapies with new antibiotics, combination therapy comprising a clinical antibiotic and a non-antibiotic agent has been considered an effective approach [13–16]. Chaves reported that *Eucalyptus camaldulensis Dehn* essential oil enhanced the activity of β-lactam antibiotics amoxicillin and ampicillin against MRSA [17]. Foxley demonstrated that branched polyethylenimine, a cationic polymer, restored the susceptibility of MRSA to β-lactam antibiotics oxacillin and ampicillin, and the synergistic antibacterial mechanism involved electrostatically binding to wall teichoic acid, thereby preventing the proper location of cell wall machinery [18,19]. Hashizume showed that the natural lipopeptide tripropeptin C revitalized β-lactam antibiotic ceftizoxime against MRSA by inhibiting β-lactamase production [20].

Inorganic nanomaterials have recently been used as antibacterial agents because such materials possess chemical stability and long lifetimes, free of bacterial resistance [21]. They are good candidates for combination therapy with antibiotics to overcome refractory MRSA infections. A nanosized ZnO coating was reported to show a synergistic antibacterial effect with gentamicin (GEN) against MRSA biofilms [22]. Silver NPs combined with traditional antibiotics also possessed synergistic antibacterial activity against MDR bacteria [23–25]. Our group found that Bi_2S_3 nanomaterials increased the antibacterial activity of GEN against MRSA [16], and the synergistic mechanism involves the destruction of bacterial membrane function, increase in antibiotic content in cytoplasm and generation of intracellular reactive oxygen species (ROS). Additionally, Bi-based and Te-based compounds have been reported to have synergistic antibacterial activity with β-lactam antibiotics [26–28]. Tellurite was reported to have synergistic antibacterial effects with cefotaxime (CTX) toward normal *Escherichia coli* by damage to proteins, DNA and other macromolecules [27,28]. Based on the synergistic antibacterial action of Bi-based and Te-based inorganic materials with antibiotics, we prepared Bi_2Te_3 NPs and investigated their anti-MRSA activity when combined with different

* Corresponding author.
E-mail address: zhonglu@wit.edu.cn (Z. Lu).

https://doi.org/10.1016/j.jinorgbio.2019.04.001
Received 10 November 2018; Received in revised form 2 April 2019; Accepted 3 April 2019
Available online 12 April 2019
0162-0134/

antibiotics. We found that Bi_2Te_3 could partially restore the antibacterial activity of β-lactam antibiotics CTX and cefuroxime (CXM). The synergistic mechanism was also investigated. To the best of our knowledge, the synergistic antibacterial effect of Bi_2Te_3 with antibiotics against MRSA has not been reported.

2. Materials and methods

2.1. Materials

Standard antibiotic disks of CTX, GEN, CXM and ciprofloxacin (CIP) were purchased from Oxoid (UK). CTX powder was purchased from Yichang Humanwell Pharmaceutical Co. Ltd. (China). 3′3-Dipropylthiadicarbocyanine ($DiSC_35$) and 2′,7′-dichlorodihydrofluorescein diacetate (DCFH-DA, ≥97%) were purchased from Sigma-Aldrich (USA). Nitrocefin was purchased from Apexbio (China). Nitrocefin disks were purchased from Becton, Dickinson and Company (USA). Mueller-Hinton (MH) broth was purchased from AoBoXing (China). All other chemicals and solvents were purchased from Sinopharm Chemical Reagent Co. Ltd. (China). MRSA strains were isolated from an infected wound of a burn patient at the laboratory of the Wuhan Third Hospital and confirmed by clinical analysis.

2.2. Synthesis of Bi_2Te_3 NPs

Spherical Bi_2Te_3 was synthesized via a simple hydrothermal process by utilizing prepared Bi_2O_3 nanospheres as bismuth precursors and templates [29]. Typically, 0.050 g Bi_2O_3 and 0.032 g TeO_2 were separately dissolved in 5 mL deionized water, and then 0.100 g $NaBH_4$ was added to the TeO_2 solution. After that, the two solutions were mixed and transferred into a Teflon-lined stainless-steel autoclave to undergo hydrothermal reaction at 150 °C for 12 h. After cooling to room temperature, the resultant product was collected by centrifugation, washed with deionized water five times and finally dried in a desiccator for a few days for further characterization. Powder X-ray diffraction (XRD) analysis was performed on a Bruker AXS D8 Discover (Cu Kα = 1.5406 Å). Scanning electron microscopy (SEM) was performed on a Hitachi S4800 microscope operating at 5.0 kV, and transmission electron microscopy (TEM) was carried out on a Philips Tecnai 20 electron microscope at an accelerating voltage of 200 kV.

2.3. Zone of inhibition test

A zone of inhibition test was used to evaluate the synergistic antibacterial activity between Bi_2Te_3 and antibiotics. A 1×10^8 colony-forming units (CFU)/mL of MRSA suspension was spread on MH agar plates. The standard antibiotic disk was gently placed on the MH agar plates and subjected to 10 μL Bi_2Te_3 solution at a concentration of 1 mg/mL. The zone of inhibition of Bi_2Te_3 alone was measured by dropping 10 μL Bi_2Te_3 solution at a concentration of 1 mg/mL on the blank disk. A standard antibiotic disk without any sample served as a control, and all experiments were performed in triplicate.

2.4. Minimal inhibitory concentration (MIC) assay

The MIC value of antibiotics or Bi_2Te_3 against MRSA was determined by a standard broth microdilution method according to the Clinical and Laboratory Standards Institute (CLSI) with slight modifications [30]. Briefly, aliquots of 1 mL of 5×10^5 CFU/mL MRSA suspension and 1 mL of serially diluted antibiotics or Bi_2Te_3 solution were incubated at 37 °C for 24 h. The MIC value was determined as the lowest concentration of antibacterial materials that could inhibit the visible growth of microorganisms.

For the drug combination test, a checkerboard method was used to evaluate the MIC of Bi_2Te_3 combined with antibiotics against MRSA. The fractional inhibition concentration (FIC) index was calculated according to the following equation [31]:

$$\text{FIC Index} = \frac{\text{MIC [A] combination}}{\text{MIC [A] alone}} + \frac{\text{MIC [B] combination}}{\text{MIC [B] alone}} \quad (1)$$

where A and B are Bi_2Te_3 and the antibiotic, respectively. The lowest FIC index is used to interpret the nature of interactions: < 0.5 shows synergism; ≥0.5 but < 1 represents partial synergism; > 1 but < 4 means an indifferent effect; and ≥4 indicates antagonism. All the determinations were performed at least in triplicate on different days.

2.5. Time kill assay

A time-kill assay was used to further explore the synergy between Bi_2Te_3 and CTX according to the CLSI method [30]. Briefly, 20 mL of 5×10^5 CFU/mL MRSA suspension was incubated with CTX, Bi_2Te_3, or a combination thereof at 37 °C with shaking at 200 rpm. At several time points, an aliquot of 20 μL of culture solution was transferred into a 24-well plate and serially diluted by an appropriate order of magnitude with phosphate buffer solution (PBS, pH 7.4). Then, 10 μL of the bacterial dilution was spread on a solid MH agar plate, and the colonies formed after 24 h of incubation at 37 °C were counted. Bacteria without the agents served as a control. The experiment was performed in triplicate.

2.6. Morphological characterization of bacteria

Field emission scanning electron microscopy (FE-SEM, Quanta 450 FEG) was used to observe the morphology of MRSA and operated at an extra high tension of 5.0 kV. Bacterial suspensions (10^8 CFU/mL) were centrifuged and washed three times with PBS. Then, the suspensions were treated with Bi_2Te_3 (8 μg/mL), CTX (32 μg/mL) or Bi_2Te_3 + CTX (8 μg/mL + 32 μg/mL) at 37 °C for 4 h with shaking at 200 rpm. Then, the bacteria were collected and washed with PBS, centrifuged at 5000 rpm for 5 min and fixed with 2.5% glutaraldehyde at 4 °C for 2 h. The specimens were washed twice with sterile water, dehydrated with a series of ethanol concentrations at 50, 75, 85, 95 and 100% for 10 min and dried under vacuum. Finally, the bacteria were coated with gold before observation. Bacteria without the agents served as a control.

2.7. Determination of cell membrane potential

Cell membrane potential was determined using the membrane potential-sensitive dye $DiSC_35$ [32]. MRSA was collected at mid-log phase and washed with 50 mM 2-[4-(2-hydroxyethyl)-1-piperazinyl] ethanesulfonic acid (HEPES) containing 5 mM glucose. Subsequently, the bacterial suspension was diluted to 10^6 CFU/mL by HEPES/glucose buffer and incubated with 0.4 μM $DiSC_35$ at 37 °C for 1 h, and then 100 mM KCl was added to balance intracellular and extracellular ion concentrations for 1 h. After that, the bacterial suspension was treated with Bi_2Te_3 (8 μg/mL), CTX (32 μg/mL) or Bi_2Te_3 + CTX (8 μg/mL + 32 μg/mL) at 37 °C for 1 h, then centrifuged at 5000 rpm for 5 min and washed with PBS three times. The fluorescence intensity was monitored by a fluorescence spectrophotometer (Hitachi F4600) at excitation and emission wavelengths of 622 and 670 nm, respectively. The experiment was performed in triplicate. Culture without the agents served as a control.

2.8. Determination of cellular potassium content

Exponentially growing bacteria were diluted to 10^6 CFU/mL with HEPES/glucose buffer and then incubated with Bi_2Te_3 (8 μg/mL), CTX (32 μg/mL) or Bi_2Te_3 + CTX (8 μg/mL + 32 μg/mL) at 37 °C for 12 h. The bacteria were collected by centrifugation at 5000 rpm for 5 min and washed with PBS three times. Then, the pellets were digested with 16 M nitric acid solution for 3 h. The cellular potassium content was measured by a flame atomic absorption spectrophotometer (Shanghai

Spectrum SP-3530). Bacteria without the agents served as a control. The experiment was performed in triplicate.

2.9. Intracellular ROS measurement

To measure intracellular ROS, bacterial cells were mixed with Bi_2Te_3 (8 μg/mL), CTX (32 μg/mL) or Bi_2Te_3 + CTX (8 μg/mL + 32 μg/mL) at 37 °C for 12 h. The samples were loaded with the fluorescent dye DCFH-DA for 30 min and then washed with PBS. The fluorescent intensity of the above samples was measured using a fluorescent spectrophotometer with excitation and emission wavelengths of 488 and 535 nm, respectively. Culture without materials served as a control. The experiment was repeated at least three times.

2.10. β-Lactamase activity

Bacterial cells (1×10^6 CFU/mL) incubated with Bi_2Te_3 (8 μg/mL), CTX (32 μg/mL) or Bi_2Te_3 + CTX (8 μg/mL + 32 μg/mL) at 37 °C for 12 h. Then, the suspensions were centrifuged at 5000 rpm for 5 min, washed with PBS three times, and then resuspended in 20 mL of PBS. The cell suspension was ultrasonicated for 30 min and then centrifuged at 5000 rpm for 5 min, and the supernatant was collected for determination of β-lactamase activity. After that, 20 μL of supernatant was dropped on a nitrocefin disk, and the color change was observed. Additionally, 10 μL of nitrocefin solution (1 mg/mL) was added into 1 mL of the supernatant, and the optical density (OD) at 492 nm was measured using ultraviolet-visible spectroscopy (722 N, INESA).

Bacterial cells (1×10^6 CFU/mL) incubated with 32 μg/mL of CTX at 37 °C for 12 h and the β-lactamase was extracted. Then 1 mL of enzyme solution mixed with 90 μL Bi_2Te_3 or sulbactam (8 and 16 μg/mL) at 37 °C for 30 min, after that 10 μL of nitrocefin solution (1 mg/mL) was added into the mixture, and the OD_{492} value was measured. Culture without materials served as a control. The experiment was performed at least in triplicate.

2.11. Quantitative real time polymerase chain reaction (qRT-PCR)

Bacterial cells (1×10^6 CFU/mL) incubated with Bi_2Te_3 (8 μg/mL), CTX (32 μg/mL) or Bi_2Te_3 + CTX (8 μg/mL + 32 μg/mL) at 37 °C for 4 h, then the bacteria were collected by centrifugation at 5000 rpm for 5 min and washed with PBS three times. The MRSA cells were digested by 4 mg/mL of lysozyme, then total RNA was isolated and purified by the Trizol reagent. The complementary DNA reverse transcription was performed according to the specification contained in the kit. The qRT-PCR amplification was performed on a qRT-PCR System (QuantStudio 6 Flex, Thermo Fisher, USA). Primers are listed in Table 1. The expression level of *blaZ* gene was normalized using 16S ribosomal RNA (*rRNA*) as an internal standard and relative messenger RNA expression was determined by the $2^{-\Delta\Delta Ct}$ method [33]. Three independent experiments were performed and each independent experiment used three replicates.

2.12. Statistical analysis

All data are expressed as the mean ± standard deviation of three experiments. Statistical analysis was performed using SPSS (IBM SPSS Statistics 24, Armonk). Data were analyzed using one-way analysis of variance (ANOVA) relative to the nontreated control. A *P*-value of < 0.05 was considered statistically significant.

Table 1
Nucleotide sequences of primers used in this study.

Gene target	Primer sequence (5′-3′)
16S rRNA [34]	F: TCCGGAATTATTGGGCGTAA R: CCACTTTCCTCTTCTGCACTCA
BlaZ [34]	F: CGTCTAAAAGAACTAGGAG R: GCTTAATTTTCCATTTGCGATAAG

3. Results and discussion

3.1. Characterization of Bi_2Te_3 NPs

Fig. 1a shows the prepared Bi_2Te_3 NPs. The diffraction peaks were well indexed to a rhombohedral Bi_2Te_3 crystal (JCPDS No. 08-27), indicative of the successful preparation of Bi_2Te_3. The SEM image (Fig. 1b) and TEM images (Fig. 1c and d) showed that the product was composed of uniform spherical particles with an average diameter of approximately 180 nm.

3.2. Antibacterial activity of Bi_2Te_3 NPs combined with antibiotics

The antibacterial activity of Bi_2Te_3 alone and combined with selected antibiotics against MRSA was assessed by a disk diffusion method and is shown in Table 2. The antibiotics CTX, CXM or CIP alone did not exhibit visible antibacterial activity against MRSA. The inhibition zone of GEN alone was 7.2 mm, which showed a weak antibacterial effect. According to the CLSI standard, MRSA is resistant to all the tested antibiotics. Bi_2Te_3 alone did not show an antibacterial effect. When Bi_2Te_3 was combined with the four antibiotics, the area of the inhibition zone was increased. Among these combinations, the area of the inhibition zone was increased by a remarkable 380% and 340% when Bi_2Te_3 was combined with CTX and CXM, respectively, which demonstrated an obvious synergistic antibacterial effect.

In order to identify which component in Bi_2Te_3 was more active in synergistic antibacterial action, we measured the antibacterial activity of water-soluble bismuth-contained compound bismuth citrate and TeO_2 NPs combined with CTX and CIP Table S1 in Supplementary Information). There was no synergistic effect against MRSA between bismuth citrate and CTX (or CIP). The only synergistic antibacterial effect was existed between TeO_2 NPs with CTX. From these results we deduced that the reactive species of Bi_2Te_3 responsible for the synergistic antibacterial effect with CTX against MRSA possibly came from the component of Te.

To further evaluate the synergistic antibacterial effect of Bi_2Te_3 combined with antibiotics against MRSA, the FIC values were measured and are shown in Table 3. The MIC value of Bi_2Te_3 alone against MRSA was > 1024 μg/mL, indicating poor antibacterial activity against MRSA. CXM, CTX and GEN alone presented MIC values of 256 μg/mL, which indicated weak antibacterial activity. When Bi_2Te_3 was combined with CXM, CTX or GEN, the MIC value decreased drastically. Among the combinations, Bi_2Te_3 and CXM had the lowest MIC values; the concentration of Bi_2Te_3 decreased from > 1024 μg/mL to 4 μg/mL, and CXM decreased from 256 to 4 μg/mL. The combination of Bi_2Te_3 and CTX showed a slightly higher MIC (32 μg/mL Bi_2Te_3 + 8 μg/mL CTX) than that of the combination of Bi_2Te_3 and CXM. GEN showed an intermediate MIC drop (from 256 to 64 μg/mL) when combined with Bi_2Te_3, and CIP presented the smallest decrease. According to the standard, synergism exists between two components when the FIC value is below 0.5. From Table 3, we know that the FIC of Bi_2Te_3 with CXM or CTX is 0.125, which indicates that a strong synergistic effect existed. The interaction between Bi_2Te_3 and GEN was also synergistic; however, the interaction was lower than that of Bi_2Te_3 with CXM or CTX. The combination of CIP with Bi_2Te_3 presented a partial synergistic effect. In our study, CXM and CTX are β-lactam class of antibiotics, and GEN and CIP belong to the aminoglycoside and quinolone classes, respectively. In our results, the synergistic effect between Bi_2Te_3 and the β-lactam class of antibiotics was stronger than that with the other selected classes of antibiotics.

To further elucidate the synergistic antibacterial activity of Bi_2Te_3 with β-lactam antibiotics, CTX was chosen to measure the time-kill

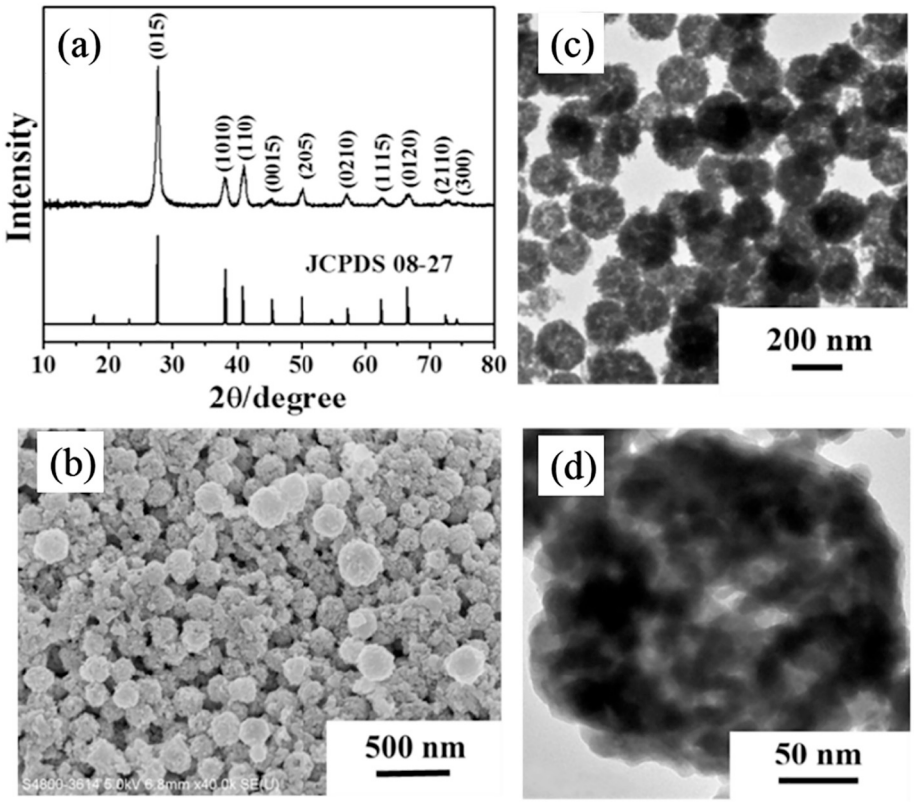

Fig. 1. XRD pattern (a), SEM image (b) and TEM images of Bi_2Te_3 (c, d).

Table 2
Inhibition zone of antibiotics in presence or absence of Bi_2Te_3 NPs against MRSA.

Agent	Antibiotic only (A), mm	Antibiotic + Bi_2Te_3 (B), mm	Increase in area[a]
CTX 30	6.0 (R)	13.2	380%
CXM 30	6.0 (R)	12.6	340%
GEN 10	7.2 (R)[b]	8.6	40%
CIP 5	6.0 (R)	7.6	60%
$Bi_2Te_3$10	6.0	–	–

[a] The percent of increase in inhibition zone area is calculated as $(B^2 - A^2) / A^2 \times 100\%$, where A and B are the inhibition zones for antibiotic only and combined with Bi_2Te_3, respectively.
[b] R resistance, according to the standard of CLSI.

Table 3
FIC index of antimicrobial combinations of Bi_2Te_3 and antibiotics against MRSA.

Agent	MIC (μg/mL)	Agents combination (μg/mL)	FIC	Interaction
CXM	256	32(CXM) + 4(Bi_2Te_3)	0.125	Synergistic
CTX	256	32(CTX) + 8(Bi_2Te_3)	0.125	Synergistic
GEN	256	64(GEN) + 32(Bi_2Te_3)	0.25	Synergistic
CIP	> 1024	512(CIP) + 64(Bi_2Te_3)	0.5	Partial synergistic
Bi_2Te_3	> 1024			

curve. As shown in Fig. 2, Bi_2Te_3 alone and CTX alone had a small effect on the growth of MRSA. When Bi_2Te_3 was combined with CTX, 6.59 log CFU/mL of MRSA was completely inactivated within 24 h. The results further demonstrated that the combination of Bi_2Te_3 and CTX had a significant synergistic effect on MRSA.

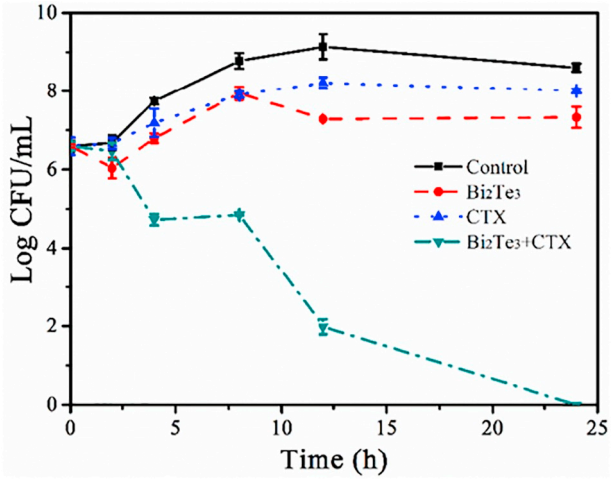

Fig. 2. Time-kill curves of MRSA treated with Bi_2Te_3, CTX and Bi_2Te_3 + CTX.

3.3. Morphology observation of MRSA

The morphologies of MRSA treated with Bi_2Te_3, CTX and the combination were observed by FE-SEM. As shown in Fig. 3a, the morphology of the untreated MRSA was intact, and the surface appeared smooth. After 6 h of treatment with CTX or Bi_2Te_3, the bacterial cells maintained integral morphology (Fig. 3b and c). However, treatment MRSA by the combination of CTX and Bi_2Te_3 caused cells obviously shrunk even disorganized and some membranes scattered (Fig. 3d). The results demonstrated that the combination could destroy the cell structure, which may be a factor for the synergistic antibacterial effect of Bi_2Te_3 and CTX.

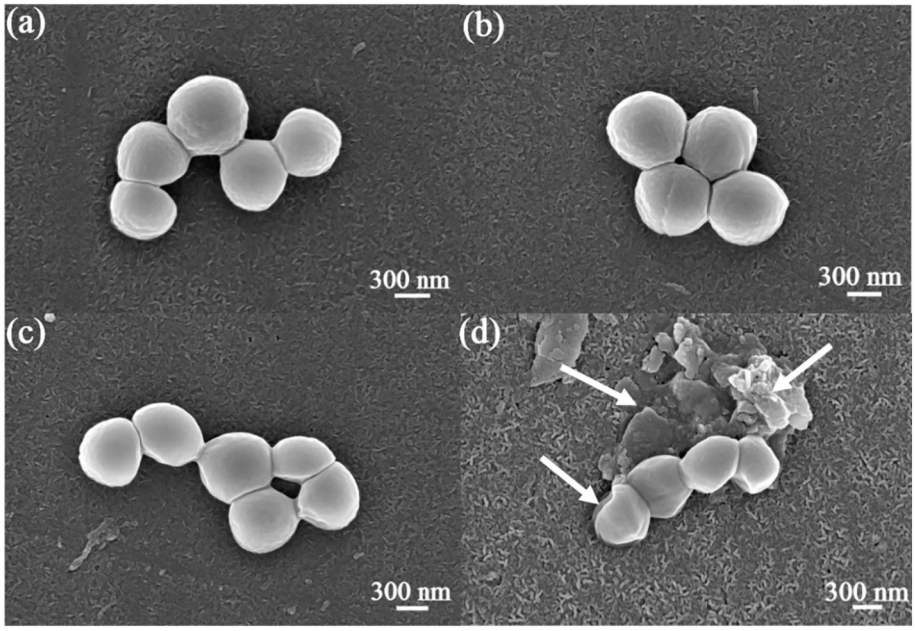

Fig. 3. FE-SEM observation of untreated MRSA (a) and after treatment by CTX (b), Bi_2Te_3 (c) and Bi_2Te_3 + CTX (d).

3.4. Influence on cell membrane

The cell membrane of bacteria acts as a barrier between the cytoplasm and extracellular media. The destruction of the bacterial cell membrane can lead to the collapse of cytoplasmic membrane potential [35]. The cytoplasmic membrane potential of MRSA after treatment with Bi_2Te_3 or CTX alone and in combination was measured using the fluorescence probe $DiSC_35$. The fluorescence of $DiSC_35$ is quenched when $DiSC_35$ partitions to an electrically polarized cell membrane. When the cytoplasmic membrane potential collapses, the probe is released back to the medium, resulting in fluorescence recovery [32,36]. As shown in Fig. 4a, the membrane potential after treatment with CTX or Bi_2Te_3 alone was almost the same as that for the control. However, the addition of the combination of Bi_2Te_3 with CTX resulted in a great increase in fluorescence, indicative of a dissipation of the membrane potential. As the membrane potential of bacteria is largely maintained by a high intracellular concentration of K^+ mediated by inward flux [37], we further examined the effects of the combination on the cellular potassium content. As shown in Fig. 4b, after incubation with CTX alone, the intracellular K^+ demonstrated no significant decrease. Bi_2Te_3 alone decreased the K^+ content by 25.29%. However, the cells treated with Bi_2Te_3 + CTX had a 63.57% decrease in K^+ content, which is more than that obtained for the simple addition of the two components. Both the results of membrane potential and intracellular K^+ content indicated that the destruction of membrane function was involved in the synergistic antibacterial action of Bi_2Te_3 with CTX.

3.5. Generation of ROS

To investigate whether ROS are associated with the synergistic antibacterial activity of Bi_2Te_3 with CTX, the intracellular ROS generation after treatment with the combination was determined by a DCFH-DA fluorescent probe. DCFH-DA can easily enter cells and be hydrolyzed by intracellular esterase to nonfluorescent 2′,7′-dichlorodihydrofluorescein (DCFH). In the presence of ROS, DCFH can be oxidized to highly fluorescent 2′,7′-dichlorofluorescein [38]. As shown in Fig. 5, cells treated with Bi_2Te_3 + CTX for 24 h presented the highest fluorescence intensity, which was 3 times higher than that obtained with CTX alone and 2 times higher than that obtained with Bi_2Te_3 alone. The results showed that the combination could greatly induce the generation of ROS in MRSA. High intracellular ROS can cause oxidative damage to biomacromolecules and further result in cell death [39].

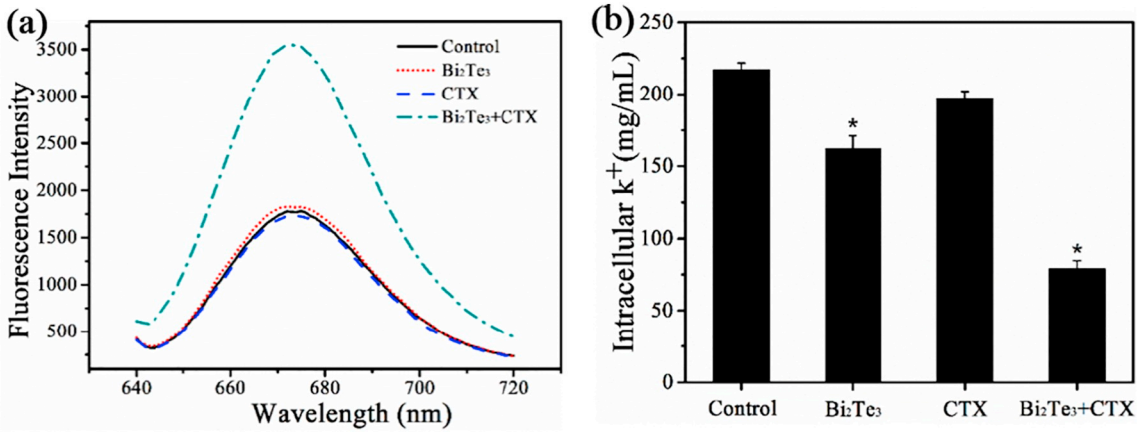

Fig. 4. Effect of Bi_2Te_3 + CTX on MRSA membrane properties. (a) Membrane potential; (b) Intracellular K^+ concentration. *Significance is confirmed by ANOVA ($p < 0.05$) compared to control group.

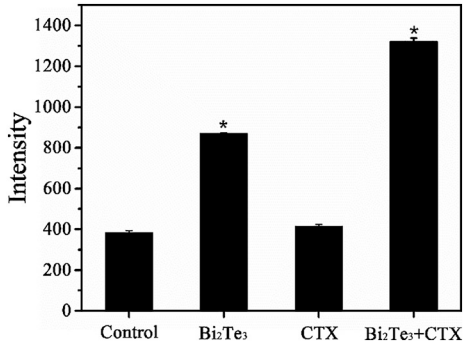

Fig. 5. Intracellular ROS of MRSA after treatment with Bi_2Te_3, CTX and Bi_2Te_3 + CTX. *Significance is confirmed by ANOVA ($p < 0.05$) compared to control group.

3.6. Inhibition of β-lactamases

β-Lactam antibiotics exert bactericidal action by interfering with the synthesis of peptidoglycan, a major component of the bacterial cell wall [40,41]. Resistant bacteria often produce β-lactamases that hydrolyze the β-lactam ring, which is essential for the bactericidal activity of the β-lactam class of antibiotics [42]. To further investigate the antibacterial mechanism, we tested the effects of Bi_2Te_3 alone and combined with CTX on β-lactamases by the nitrocefin disk assay. Nitrocefin, containing a β-lactam ring, is often used to rapidly detect β-lactamase [43,44]. Usually, β-lactamases hydrolyze the β-lactam ring of nitrocefin, resulting in a color change from yellow to red [45]. As shown in Fig. 6a, the incubation of a nitrocefin disk with Bi_2Te_3 resulted in a yellow color, which indicated no or little β-lactamase in MRSA. Incubation of the disk with CTX resulted in a dark red color, which revealed much more β-lactamase production. However, incubation with the combination of Bi_2Te_3 and CTX generated less β-lactamase than did incubation with CTX. We further measured β-lactamase content by a nitrocefin solution method. When nitrocefin is hydrolyzed by β-lactamase, the maximum absorption peak is changed from 390 nm to 480 nm [45]. As shown in Fig. 6b, incubation of MRSA with CTX caused a high OD_{492} value of the nitrocefin solution, which indicated high β-lactamase generation. However, the incubation of MRSA with Bi_2Te_3 + CTX resulted in a decrease in the enzyme. The results demonstrated that CTX alone induced more β-lactamase generation by MRSA; this enhanced production could hydrolyze the β-lactam ring of CTX and cause the antibiotic to be ineffective. The combination of Bi_2Te_3 with CTX decreased β-lactamase, therefore further decreasing the hydrolysis of β-lactam antibiotics, which caused CTX to be partially reactivated for the inhibition of MRSA.

As the decrease of β-lactamases may come from the inactivation or less generation, we next investigated which one responsible for this decrease. MRSA were cultured with CTX to induce more generation of β-lactamases, and the enzyme activity was measured after mixed with Bi_2Te_3 and compared with that of sulbactam, an inhibitor of β-lactamases [46]. As shown in Fig. 6c, sulbactam significantly inactivated the β-lactamases, however Bi_2Te_3 nanoparticle almost unchanged the β-lactamases activity, which indicated that the inactivation was not responsible for the decrease of β-lactamases caused by Bi_2Te_3 and CTX treatment. We further investigated the expression of β-lactamases-related *blaZ* gene by qRT-PCR after treatment MRSA with the combination of Bi_2Te_3 and CTX and the results are plotted in Fig. 6d. CTX alone induced MRSA to produce more *blaZ* gene, however, after treatment with Bi_2Te_3 + CTX, the expression of *blaZ* gene reduced > 44.7%. Considering the combination Bi_2Te_3 with CTX had no synergistic antibacterial effect against β-lactamase negative *Staphylococcus aureus* (*S. aureus*, ATCC 6538) (Fig. S1 in Supplementary Information), the synergistic effect partly derived from decreasing the generation of β-lactamase.

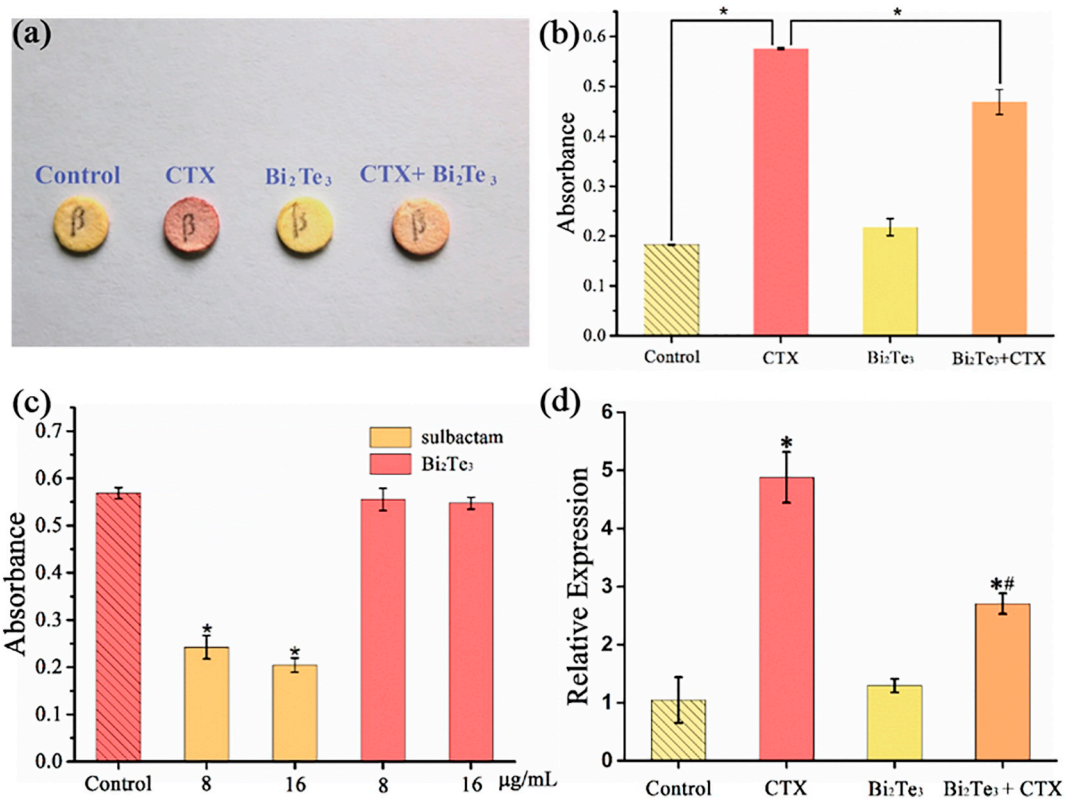

Fig. 6. Changes of β-lactamases (a–c) and *blaZ* gene (d) after treatment by CTX, Bi_2Te_3 and combination. *Significantly different ($P < 0.05$) from control and CTX + Bi_2Te_3 group. #Significantly different ($p < 0.05$) from CTX.

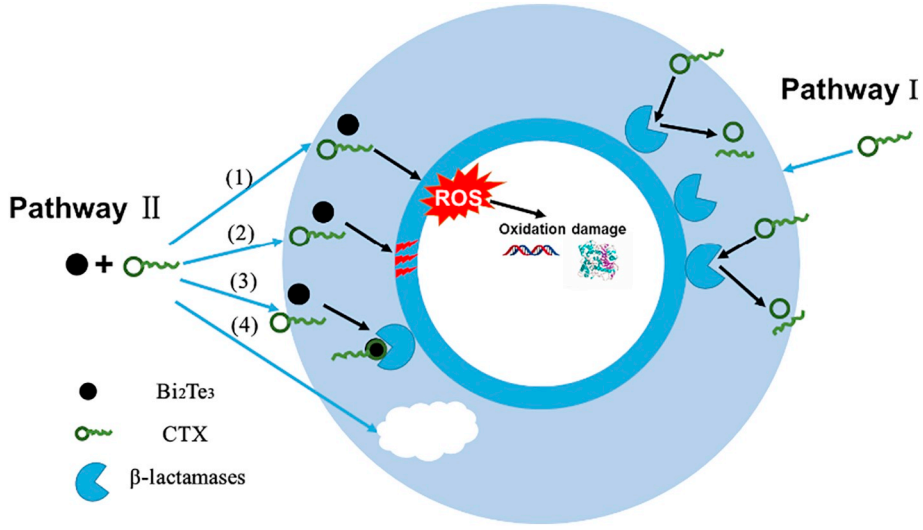

Fig. 7. Schematic drawing of the synergistic antibacterial pathway of Bi_2Te_3 with CTX against MRSA. Pathway I is not effective due to antibiotic-resistance by MRSA and pathway II is the major pathway leading to cell death.

3.7. Summary of synergistic antibacterial mechanism

As shown in our results and other reports [47,48], β-lactam antibiotics can induce MRSA to produce β-lactamases, which degrade the β-lactam class of antibiotics and make such antibiotics ineffective against MRSA (Fig. 7, Pathway I). The mechanism by which Bi_2Te_3 NPs partially revived CTX was proposed as shown in pathway II in Fig. 7: (1) CTX combined with Bi_2Te_3 induces the generation of more intracellular ROS, which oxidize the biomacromolecular components of bacteria. (2) The combination destroys the membrane function of bacteria. (3) The combination partially inhibits the production of β-lactamases induced by CTX. (4) The combination causes direct destruction of the cell structure.

4. Conclusions

In summary, the antibacterial activity of the β-lactam antibiotic CTX against MRSA was partially revived by combination with Bi_2Te_3 NPs. The synergistic mechanism involves the destruction of bacterial membrane function, generation of intracellular ROS, direct destruction of cell structure and partial inhibition of the production of β-lactamases. This combination could potentially be exploited for new strategies to inhibit MRSA.

Abbreviations

ANOVA	Analysis of variance
CTX	Cefotaxime
CXM	Cefuroxime
CLSI	Clinical and Laboratory Standards Institute
CIP	Ciprofloxacin
CFU	Colony-forming units
DCFH	2′,7′-Dichlorodihydrofluorescein
DCFH-DA	2′,7′-Dichlorodihydrofluorescein diacetate
$DiSC_35$	3′3-Dipropylthiadicarbocyanine
FE-SEM	Field emission scanning electron microscopy
FIC	Fractional inhibition concentration
GEN	Gentamicin
HEPES	2-[4-(2-hydroxyethyl)-1-piperazinyl] ethanesulfonic acid
MRSA	Methicillin-resistant *Staphylococcus aureus*
MIC	Minimal inhibitory concentration
MH	Mueller-Hinton
MDR	Multidrug-resistant
NPs	Nano particles
OD	Optical density
PBS	Phosphate buffer solution
qRT-PCR	Quantitative real time polymerase chain reaction
ROS	Reactive oxygen species
rRNA	Ribosomal RNA
SEM	Scanning electron microscopy
S. aureus	*Staphylococcus aureus*
TEM	Transmission electron microscope
XRD	X-ray diffraction

Acknowledgement

This work was supported by the National Natural Science Foundation of China (21371139) and the Graduate Innovation Foundation of Wuhan Institute of Technology (CX2017087).

Appendix A. Supplementary data

Supplementary data to this article can be found online at https://doi.org/10.1016/j.jinorgbio.2019.04.001.

References

[1] Y. Tang, L. Fang, C. Xu, Q. Zhang, Anim. Health Res. Rev. 18 (2017) 1–12.
[2] B.D. Brooks, A.E. Brooks, Adv. Drug Deliv. Rev. 78 (2014) 14–27.
[3] R. Laxminarayan, A. Duse, C. Wattal, A.K. Zaidi, H.F. Wertheim, N. Sumpradit, E. Vlieghe, G.L. Hara, I.M. Gould, H. Goossens, Lancet Infect. Dis. 13 (2013) 1057–1098.
[4] K.A. Davis, J.J. Stewart, H.K. Crouch, C.E. Florez, D.R. Hospenthal, Clin. Infect. Dis. 39 (2004) 776–782.
[5] F.R. DeLeo, M. Otto, B.N. Kreiswirth, H.F. Chambers, Lancet 375 (2010) 767–768.
[6] C.U. Koeser, M.T.G. Holden, M.J. Ellington, E.J.P. Cartwright, N.M. Brown, A.L. Ogilvy-Stuart, L.Y. Hsu, C. Chewapreecha, N.J. Croucher, S.R. Harris, M. Sanders, M.C. Enright, G. Dougan, S.D. Bentley, J. Parkhill, L.J. Fraser, J.R. Betley, O.B. Schulz-Trieglaff, G.P. Smith, S.J. Peacock, New Engl. J. Med. 366 (2012) 2267–2275.
[7] S. Monecke, G. Coombs, A.C. Shore, D.C. Coleman, P. Akpaka, M. Borg, H. Chow, M. Ip, L. Jatzwauk, D. Jonas, K. Kadlec, A. Kearns, F. Laurent, F.G. O'Brien, J. Pearson, A. Ruppelt, S. Schwarz, E. Scicluna, P. Slickers, H.-L. Tan, S. Weber, R. Ehricht, PLoS One 6 (2011) e17936.
[8] J.C. Lin, G. Aung, A. Thomas, M. Jahng, S. Johns, J. Fierer, J. Infect. Chemother. 19 (2013) 42–49.
[9] S. Donadio, S. Maffioli, P. Monciardini, M. Sosio, D. Jabes, J. Antibiot. 63 (2010) 423–430.
[10] K. Lewis, Nat. Rev. Drug Discov. 12 (2013) 371–387.
[11] G. Taubes, Science 321 (2008) 356–361.
[12] C.A. Arias, B.E. Murray, New Engl. J. Med. 372 (2015) 1168–1170.
[13] L. Czaplewski, R. Bax, M. Clokie, M. Dawson, H. Fairhead, V.A. Fischetti, S. Foster,

B.F. Gilmore, R.E. Hancock, D. Harper, Lancet Infect. Dis. 16 (2016) 239–251.
[14] L. Ejim, M.A. Farha, S.B. Falconer, J. Wildenhain, B.K. Coombes, M. Tyers, E.D. Brown, G.D. Wright, Nat. Chem. Biol. 7 (2011) 348–350.
[15] R. C. Moellering, Jr., New Engl. J. Med. 363 (2010) 2377–2379.
[16] L. Ma, J. Wu, S. Wang, H. Yang, D. Liang, Z. Lu, J. Inorg. Biochem. 168 (2016) 38–45.
[17] T.P. Chaves, R.E.E. Pinheiro, E.S. Melo, M.J.d.S. Soares, J.S.N. Souza, T.B.d. Andrade, T.L.G.d. Lemos, H.D.M. Coutinho, Ind. Crop. Prod. 112 (2018) 70–74.
[18] M.A. Foxley, S.N. Wright, A.K. Lam, A.W. Friedline, S.J. Strange, M.T. Xiao, E.L. Moen, C.V. Rice, ACS Med. Chem. Lett. 8 (2017) 1083–1088.
[19] M.A. Foxley, A.W. Friedline, J.M. Jensen, S.L. Nimmo, E.M. Scull, J.B. King, S. Strange, M.T. Xiao, B.E. Smith, K.J. Thomas Iii, D.T. Glatzhofer, R.H. Cichewicz, C.V. Rice, J. Antibiot Tokyo. 69 (2016) 871–878.
[20] H. Hashizume, Y. Takahashi, T. Masuda, S.I. Ohba, T. Ohishi, M. Kawada, M. Igarashi, J. Antibiot Tokyo. 71 (2017) 79–85.
[21] A.M. Allahverdiyev, K.V. Kon, E.S. Abamor, M. Bagirova, M. Rafailovich, Expert. Rev. Anti-Infe. 9 (2011) 1035–1052.
[22] M.M. Alves, O. Bouchami, A. Tavares, L. Cordoba, C.F. Santos, M. Miragaia, M. de Fatima Montemor, ACS Appl. Mater. Interfaces 9 (2017) 28157–28167.
[23] H. Deng, D. McShan, Y. Zhang, S.S. Sinha, Z. Arslan, P.C. Ray, H. Yu, Environ. Sci. Technol. 50 (2016) 8840–8848.
[24] D. Mcshan, Y. Zhang, H. Deng, P.C. Ray, H. Yu, J. Environ. Sci. Health C Environ. Carcinog. Ecotoxicol. Rev. 9 (2015) 360–366.
[25] R. Thomas, A.P. Nair, K.R. Soumya, J. Mathew, E.K. Radhakrishnan, Appl. Biochem. Biotechnol. 173 (2014) 449–460.
[26] R. Wang, T.P. Lai, G. Peng, H. Zhang, P.L. Ho, C.Y. Woo, G. Ma, Y.T. Kao, H. Li, H. Sun, Nat. Commun. 9 (2018) 439–451.
[27] R.C. Molina-Quiroz, D.E. Loyola, C.M. MunOz-Villagrán, R. Quatrini, C.C. Vásquez, J.M. Pérez-Donoso, PLoS One 8 (2013) e79499.
[28] R.C. Molina-Quiroz, C.M. Muñoz-Villagrán, E. de la Torre, J.C. Tantaleán, C.C. Vásquez, J.M. Pérez-Donoso, PLoS One 7 (2012) e35452.
[29] F. Qin, H. Zhao, G. Li, H. Yang, J. Li, R. Wang, Y. Liu, J. Hu, H. Sun, R. Chen, Nanoscale 6 (2014) 5402–5409.
[30] Clinical and Laboratory Standards Institute, Performance Standards for Antimicrobial Susceptibility Testing: Twenty-First Informational Supplement Document M100-S23, CLSI, Wayne, PA, 2013.
[31] A. Duarte, S. Ferreira, F. Silva, F.C. Domingues, Phytomedicine 19 (2012) 236–238.
[32] X. Wang, Q. Han, N. Yu, T. Wang, C. Wang, R. Yang, Colloids Surf. B. 162 (2018) 296–305.
[33] S. Wang, Q. Huang, X. Liu, Z. Li, H. Yang, Z. Lu, ACS Biomater. Sci. Eng. (2019), https://doi.org/10.1021/acsbiomaterials.9b00118.
[34] X. Liu, P.J. Pai, W. Zhang, Y. Hu, X. Dong, P.Y. Qian, D. Chen, H. Lam, Sci. Rep. 6 (2016) 19841.
[35] Zhou, Kang, Zhou, Wei, Li, Pinglan, Liu, Guorong, Zhang, Jinlan, Food Control. 19 (2008) 817–822.
[36] K. Nüsslein, L. Arnt, J. Rennie, C. Owens, G.N. Tew, Microbiology 152 (2006) 1913–1918.
[37] P.A. Lambert, S.M. Hammond, Biochemical. Bioph. Res. Co. 54 (1973) 796–799.
[38] H. Wang, J.A. Joseph, Free Radical Bio. Med. 27 (1999) 683.
[39] M.A. Kohanski, D.J. Dwyer, B. Hayete, C.A. Lawrence, J.J. Collins, Cell 130 (2007) 797–810.
[40] T.F. Durand-Reville, S. Guler, J. Comita-Prevoir, B. Chen, N. Bifulco, H. Huynh, S. Lahiri, A.B. Shapiro, S.M. McLeod, N.M. Carter, S.H. Moussa, C. Velez-Vega, N.B. Olivier, R. McLaughlin, N. Gao, J. Thresher, T. Palmer, B. Andrews, R.A. Giacobbe, J.V. Newman, D.E. Ehmann, B. de Jonge, J. O'Donnell, J.P. Mueller, R.A. Tommasi, A.A. Miller, Nat. Microbiol. 2 (2017) 17104–17114.
[41] J. Chu, X. Vila-Farres, D. Inoyama, M. Ternei, L.J. Cohen, E.A. Gordon, B.V. Reddy, Z. Charlop-Powers, H.A. Zebroski, R. Gallardo-Macias, M. Jaskowski, S. Satish, S. Park, D.S. Perlin, J.S. Freundlich, S.F. Brady, Nat. Chem. Biol. 12 (2016) 1004–1006.
[42] S.S. Tang, A. Apisarnthanarak, L.Y. Hsu, Adv. Drug Deliv. Rev. 78 (2014) 3–13.
[43] K.E. Boehle, C.S. Carrell, J. Caraway, C.S. Henry, ACS Sensors 3 (2018) 1299–1307.
[44] F. Duan, X. Feng, Y. Jin, D. Liu, X. Yang, G. Zhou, D. Liu, Z. Li, X.J. Liang, J. Zhang, Biomaterials 144 (2017) 155–165.
[45] C.H. O'Callaghan, A. Morris, S.M. Kirby, A.H. Shingler, Antimicrob. Agents Ch. 1 (1972) 283–288.
[46] S.M. Drawz, R.A. Bonomo, Clin. Microbiol. Rev. 23 (2010) 160–201.
[47] K.M. O'Connell, J.T. Hodgkinson, H.F. Sore, M. Welch, G.P. Salmond, D.R. Spring, Angew. Chem. Int. Edit. 52 (2013) 10706–10733.
[48] J.F. Fisher, S.O. Meroueh, S. Mobashery, Cheminform 36 (2005) 395–424.